energies

MDPI

Article

Force and Motion Characteristics of Contamination Particles near the High Voltage End of UHVDC Insulator

Lei Lan, Gongda Zhang, Yu Wang * and Xishan Wen

School of Electrical Engineering, Wuhan University, Wuhan 430072, China; lanlei@whu.edu.cn (L.L.); zhanggongda@whu.edu.cn (G.Z.); xswen@whu.edu.cn (X.W.)

* Correspondence: yuwang@whu.edu.cn; Tel.: +86-27-6877-2285

Received: 30 March 2017; Accepted: 7 July 2017; Published: 11 July 2017

Abstract: It is important to reveal the relations of physical factors to deposition of contaminants on insulator. In this paper, the simulation model of high voltage end of insulator was established to study the force and motion characteristics of particles affected by electric force and airflow drag force near the ultra-high voltage direct current (UHVDC) insulator. By finite element method, the electric field was set specially to be similar to the one near practical insulator, the steady fluid field was simulated. The electric force and air drag force were loaded on the uniformly charged particles. The characteristics of the two forces on particles, the relationship between quantity of electric charge on particles and probability of particles contacting the insulator were analyzed. It was found that, near the sheds, airflow drag force on particles is significantly greater than electric force with less electric charge. As the charge multiplies, electric force increases linearly, airflow drag force grows more slowly. There is a trend that the magnitude of electric force and drag force is going to similar. Meanwhile, the probability of particles contacting the insulator is increased too. However, at a certain level of charge which has different value with different airflow velocity, the contact probability has extremum here. After exceeding the value, as the charge increasing, the contact probability decreases gradually.

Keywords: electric force; air drag force; uniform charged; contact probability; contamination particle; multi-physics field

1. Introduction

The state of outdoor polluted insulation is closely related to the normal operation of power systems [1]. The deposition of contaminants on insulator surface is affected by various physical effects. Some studies have been done concerning outdoor insulation pollution for preventing and reducing operation accident caused by pollution flashover [2,3]. Some research on insulator structure and operation performance has pointed out that composite insulator has great advantages over porcelain and glass insulator in the UHVDC system. The structure of composite sheds is closely related to the DC pollution flashover characteristics, the parameters of the shed affects the partial discharge on shed surface and flashover voltage [4,5]. Aerodynamic structure of the shed can play a role in reducing insulator pollution and improving wet discharge voltage [6].

The precondition of flashover is the existing of contamination layer on the surface of the insulator, and related with other factors, such as humidity, temperature, and weather conditions [7–9], which is a very complex physical process. The motion of contamination particles in atmosphere is affected by air drag force, electric force, collision force, and other forces. To analysis the forces on the contaminant particles is helpful to reveal the physical process and the laws of insulator contamination, to offer more effective antifouling measures, and to improve the design of the insulator.

With respect to the analysis of the motion of contamination particles near the insulator, Ye et al. [10] established the dynamic model under the condition of low wind speed based on the theory of fluid mechanics and two-phase flow, and studied the force characteristics of the contamination particles near the insulator under the condition of low wind speed. On the basis of flow field around insulators simulated by the method of computational fluid dynamics, Jiang et al. [11] analyzed the effects of free stream velocity, diameter of particles, and angle of the free stream on the collision coefficient of contamination particles. Sun et al. [12] built a high-speed railway insulator simulation model, and analyzed the force situation of contamination particles in high speed airflow. The relationships of the pollution degree characterized by the volume fraction of the contamination on the shed upper or lower surface with airflow velocity, and angle of airflow were declared. However, none of the above simulation studies was concerned with the effect of electric field force on the motion of contamination particles.

By some coaxial electrode model experiments and two-dimension axial symmetric electrode simulation, it is indicated that the charged dust particles deflect along the electric field line driven by the electric force, the drag force dominates and the particles move with the strong wind [13]. Sun et al. [14] pointed out that the contamination on insulator is greatly affected by electric field, and is more serious under DC voltage than AC voltage from the experiment phenomenon of contamination tests of insulator in a small dust chamber. Liu [15] discussed the movement direction of fog particles in ionized field around HVDC transmission line, and studied the polarity of fog particles and motion characteristics in ionized field by the experiments, similarly to the works of Wang et al. [13]. Ravelomanantsoa [16,17] raised an experiment similar to wind tunnel test to study the accumulation of road salt on the energized insulator, involved the factors of air flow velocity and salt particle diameter. From the results of experiment and calculation of scale model insulator, it was indicated that the factor airflow has the greatest influence on particle motion; the electric force causes the deflection of contamination particles as moving between the sheds [18]. Olsen [19] considered the effects of airflow drag force, the electric force and gravity in the calculation of particle trajectories and contaminant distribution on insulator string which is a cylinder model.

In the present studies mentioned above, the relationships between contamination particle movement, pollution situation, fluid field, and electric field were discussed from the two approaches of simulation and experiment. However, the quantitative analysis of the relationship between the motion of contamination particles, fluid field, and the electric field near the practical insulator is not involved. In this paper, the electric field near the high voltage end of insulator under the operating environment was taken as the background electric field; the quantitative effects of airflow drag force and electric charge on contamination particle motion were analyzed with the condition of low airflow velocity.

2. Analysis of Forces on Contamination Particles near Insulator

It is necessary to clarify the forces on contamination particles in the study of motion of natural contaminants. According to the difference of material form, the contamination particle is considered as dispersed solid phase, and the air is a continuous gas phase, the surface of the insulator is the fluid–wall boundary [11,20,21]. The volume fraction of dust particles in the atmosphere is very small, which is sparse discrete phase, the effect of the particles on the air flow and the interaction between particles can be neglected [10,22].

The forces on the contaminant particle moving near the insulator can be classified into two types: the force produced by fluid flow and the force produced by external physical field. The fluid forces include drag force, Magnus spin lift force, Saffman shear lift force, pressure gradient force, and so on. Wherein, the drag force has a most important role, the other forces are too small to be considered in the motion. The external physical field forces include gravity, polarization force, electric force and magnetic force, etc. Because the high intensity of the electrical field near the high voltage end of insulator, the effect of electric force on contamination particles should be considered while neglecting the effect of very small polarization force [13,23].

2.1. Air Drag Force

As a single spherical particle moving in the atmosphere, the drag force can be expressed as [23]

$$F_D = \frac{1}{2} C_D A_p \rho u_p^2 = \frac{1}{8} C_D \pi d_p^2 \rho u_p^2, \quad (1)$$

where C_D is the drag coefficient, u_p is the velocity of spherical particle relative to fluid, A_p and d_p are the projection area and diameter of spherical particle, ρ is the fluid density.

The drag coefficient C_D is related to Reynolds number Re which is the ratio of inertia force and viscous force in physics. There is a complex airflow field near the insulator, and the Reynolds number has a spatial distribution. When the spatial position of the particle is changed, the air drag force is very different. Therefore, the acting of drag force on contamination particle is a transient process, the magnitude and direction of the drag force could be calculated according to a certain time and position.

2.2. Electric Force

In the electric field, especially the DC ionized field, the contaminant particles are charged during moving. A majority of charged particles by field charging in atmosphere have a diameter size between 1 μm and 100 μm whose ratio is about 90% [11,13]. Saturated quantity of electric charge on each particle can be calculated as [24]

$$q_{ps} = \frac{3\varepsilon_r}{\varepsilon_r + 2} \varepsilon_0 \pi {d_p}^2 E_p, \quad (2)$$

where E_p is the maximum external electric field density as the particle has saturated charges in the non-uniform electric field, d_p is particle diameter, ε_r is the relative permittivity of particle, ε_0 is the permittivity of free space. The E_p is distributed in space; the particles in a non-uniform electric field have different saturated charge. In considering a small range of particle charges, to reduce the complexity of analysis, it can be considered that E_p has a uniform value.

The particle has saturated charges, the electric force F_e is

$$F_e = q_{ps} E_0, \quad (3)$$

where E_0 is the background electric field density at the position where the charged particle is.

2.3. Gravity

For spherical particle, the gravity on it can be expressed as

$$F_g = \frac{1}{6} \pi {d_p}^3 \rho_p g, \quad (4)$$

where ρ_p is particle mass density, g is gravity acceleration.

The motion equation of contamination particle near insulator combined air drag force, electric force, and gravity can be expressed as

$$\frac{1}{6} \pi {d_p}^3 \rho_p \frac{dv}{dt} = F_D + F_e + F_g, \quad (5)$$

where v is the moving velocity of particles relative to the ground.

3. Simulation

The drag force and electric field force is the parameters changing with time and space, thus the three dimension simulation is essential for studying the contamination particles motion. The finite element method was applied in the simulations of the electric and fluid fields. The forces on the

particles are derived from the mechanical action of the electric field and flow field on the dispersed phase particle. Particle trajectory and motion state can be calculated by forces.

3.1. The Model and Calculate Condition

The study object is the contaminant particles moving around the high voltage end of the ±800 kV composite insulator. Referring to the practical insulator with a length of 10.2 m, creepage distance is 35.1 m [25], the simulation model of high voltage end was built after simplifying some fittings and details of sheds. It is shown in Figure 1. The simplified model is 1 m full length—which has a 0.2 m metal joint and a 0.8 m insulate rod with 50 mm diameter—only has sheds at the high voltage end in which the bigger shed diameter is 246 mm; the middle shed diameter is 186 mm. The spherical particles were used to simulate the contaminant dust [20]. From the contamination data in the field [26], the contamination particles with diameter is 20 μm accounts for the majority of the contamination samples, and the major component of insoluble matter is SiO_2. So, the physics parameters of contaminant particles were that the particle diameter is 20 μm, the bulk density of SiO_2 is 2200 kg/m^3, the relative permittivity is 4 [27].

The insulator string and the surrounding space are symmetrical. In order to save the computing resources, the geometry and the calculation domain are built up with the 1/2 part based on the axial section of insulator. The background electric field near the high voltage end of the insulator was established which is similar with the one around the ±800 kV composite suspension insulator [25]. The distribution of electric field intensity is shown in Figure 2.

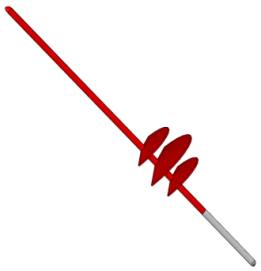

Figure 1. The high voltage end simplified model of composite insulator.

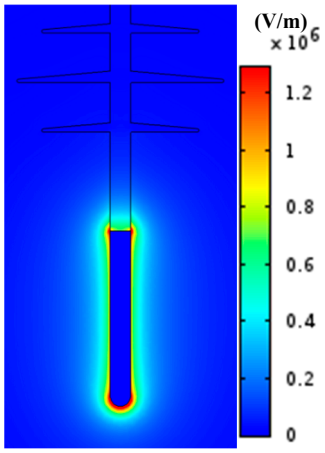

Figure 2. The high voltage end simplified model of composite insulator.

In the fluid field simulation, Reynolds average Navier–Stokes equation (RANS) and *k*-ε turbulence model were applied [21]. The initial airflow velocity at inlet was set to 1, 2, 3, and 5 m/s, and the direction was perpendicular to the insulator axial. The outlet condition was zero pressure diffusion.

In the component of particle tracing for fluid flow, the release velocity of particles was consistent with the airflow velocity in turbulent flow component; the electric force and drag force were added as the factors affect the particle motion in the component. The state of particle when contacting the surface of the insulator can be described in that it sticks to the contact position, and motion parameters maintain the value at the moment of contact, and it can be called as frozen.

All particles were charged uniformly, and the charge on each particle reached saturation value as the E_p was set to 200 kV/m. The polarity of space charges in the vicinity of conductor of the DC transmission line is similar to the conductor's, and the charged particles have the same polarity as the high voltage end of the insulator [15,28,29]. A transient solution was applied to simulate the particle tracing. The simulation time was 1 s, and time step was 0.01 s.

There were three components be used for simulation modeling. Firstly, the electric field near high voltage end of insulator was calculated in the electrostatics component, the data of electric field were used as values of variables not solved in the static turbulence study. Secondly, the turbulent flow component was used to simulate fluid field. As the things above mentioned, the data of electric field and fluid field were saved in the static turbulence study. Thirdly, for studying the moving processes of contamination particles, the component of particle tracing for fluid flow was applied to calculate the motion state of particles with the gravity, drag force, and electric force which was taken from static turbulence study. The particle charge was set as a particle property in particle tracing component calculated by Formula (2) when a value of E_p was specified.

3.2. Simulation Results

When the airflow entrance velocity V_0 was 3 m/s, the airflow velocity distribution near the insulator model is shown in Figure 3. There was a small area of airflow deceleration zone on the windward side of insulator, the airflow velocity in the vicinity of insulator was less than the entrance velocity. There was a wide range of low velocity zones on the leeward side, but the air velocity increased gradually as airflow was moving away from the insulator.

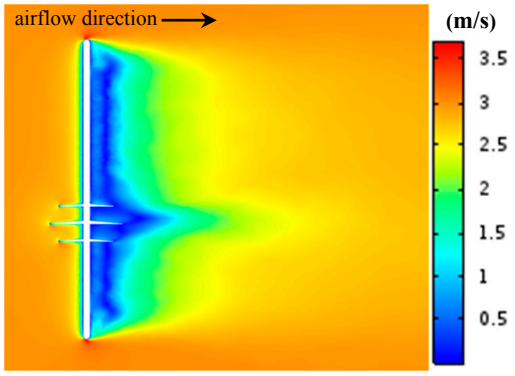

Figure 3. The contour map of airflow velocity in the insulator axial section.

Considering the particles had been charged saturated which still had a certain distance away from sheds. The saturated charge on single particle was 4.4505×10^{-15} C which is set to 1 p.u., as E_p = 200 kV/m. The time of releasing contamination particles from entrance is 0 s. A majority of particles had arrived at the leeward side of sheds after 0.4 s with the help of gravity, electric force, and airflow drag force, a part of them were frozen when contacting the sheds. At this moment, the position of contamination particles is shown in Figure 4. The distribution of the contamination particles on the sheds as the charge Q on single particle was 1, 10, 30, and 50 p.u. is shown in Figure 5. The most of particles contacted to sheds were frozen on the lower surface, and a few of them were stay on the edge of sheds. It is revealed that the contaminants tend to accumulate on the lower surface of sheds at the high voltage end of insulator. This phenomenon is similar with the practical contamination

characteristics and distribution of DC insulators [30–32]. Similarly to the simulation results of this paper, in another study of contamination particle deposit characteristics considering the effects of electric force and air drag force with neglecting turbulent flow, the researchers in the theory analysis pointed out that the charged particles which have same polarity with conductors, deflected and hit the lower insulator surface as sweeping past the insulator.. In their scale model experiment, the deposition phenomenon of the bottom surface of sheds occurred [33].

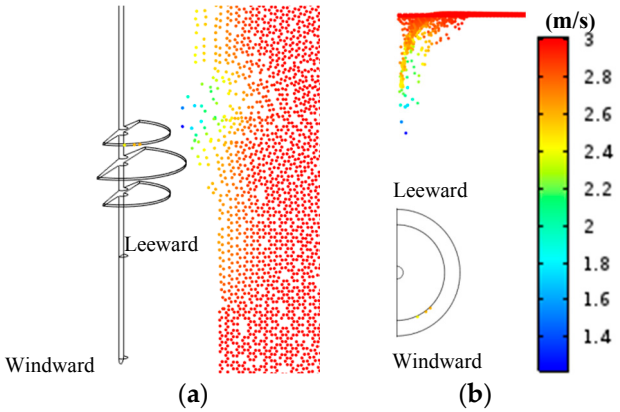

Figure 4. The map of contamination particles movement position from (**a**) aerial view and (**b**) top view after being released for 0.4 s.

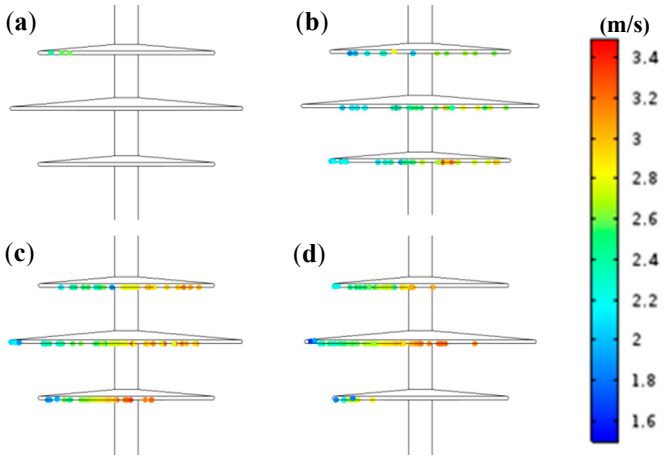

Figure 5. The distribution map of contamination particles frozen on insulator surface, when (**a**) Q = 1 p.u.; (**b**) Q = 10 p.u.; (**c**) Q = 30 p.u.; and (**d**) Q = 50 p.u.

4. Analysis of Characteristics of Forces and Motion

A rectangular plane that is perpendicular to windward, 604 cm^2, was drawn. All force data of each particle in this plane were extracted for analyzing the characteristics of forces on particles closed to the sheds.

4.1. Characteristics of Air Drag Force and Electric Force

When airflow entrance velocity V_0 was 3 m/s, the single particle charge was 1 p.u., the direction of air drag force and electric force on particles which moved to the front of the bigger shed edge at 0.19 s after release are shown in Figure 6, and those that moved to the back of the sheds at 0.28 s after release are shown in Figure 7. From the figures, it is observed that the direction of electric force has obvious regularity which always departs from the high voltage end of insulator. The electric force plays a role in slowing down the contamination particles on the windward side of insulator,

and accelerates particles moving away on the leeward. However, the direction of air drag force does not have obvious regularity, it is closely related to the turbulence, electric field distribution and other factors. So it is difficult to quantify the particle motion characteristics from the direction regularity of air drag force.

It can be seen that the drag force increased remarkably when the particles moved to the place be apart from the edge of bigger shed 0.16 m. So it is inferred that the turbulence and electric field close to the insulator play more important roles in the particle motion from here. In order to study the numerical relationship between drag force and electric force, the values of forces on each particle were extracted to plot a series of curves. These curves are shown in Figure 8. The electric force and drag force curves were plotted respectively when particles have a different charge Q. On condition that the charge Q was 1 p.u., the drag force was higher than the electric force about 0.4 to 0.5 orders of magnitude from the statistical data. With Q increasing from 1 p.u. to 10 p.u., the drag force and electric force on particles were increased overall, nevertheless, the electric force increased more greatly than the drag force. When Q > 30 p.u., the magnitude curves of drag force and electric force became more and more similar. The electric force played a more important role to affect the motion of particles than the drag force, and the magnitude of them tended to equilibrium gradually.

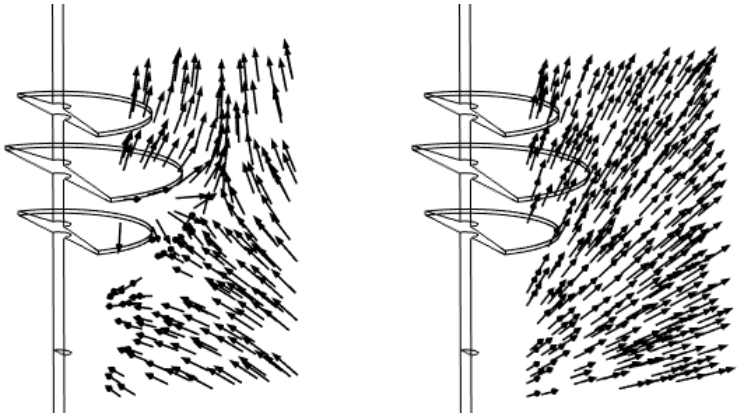

(**a**) (**b**)

Figure 6. The direction map of (**a**) air drag force and (**b**) electric force on particles at 0.19 s after release.

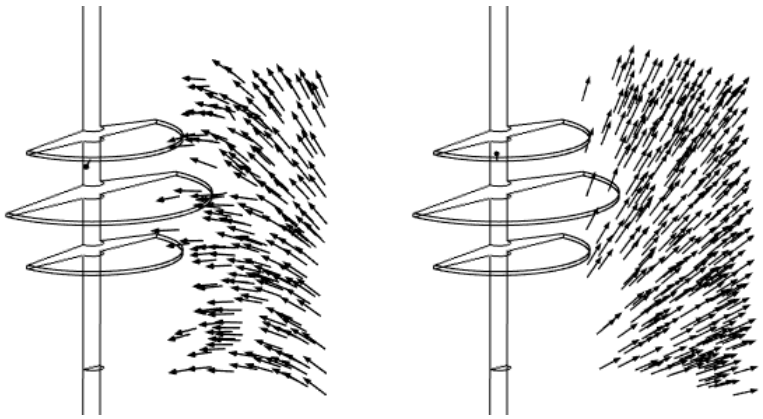

(**a**) (**b**)

Figure 7. The direction map of (**a**) air drag force and (**b**) electric force on particles at 0.28 s after release.

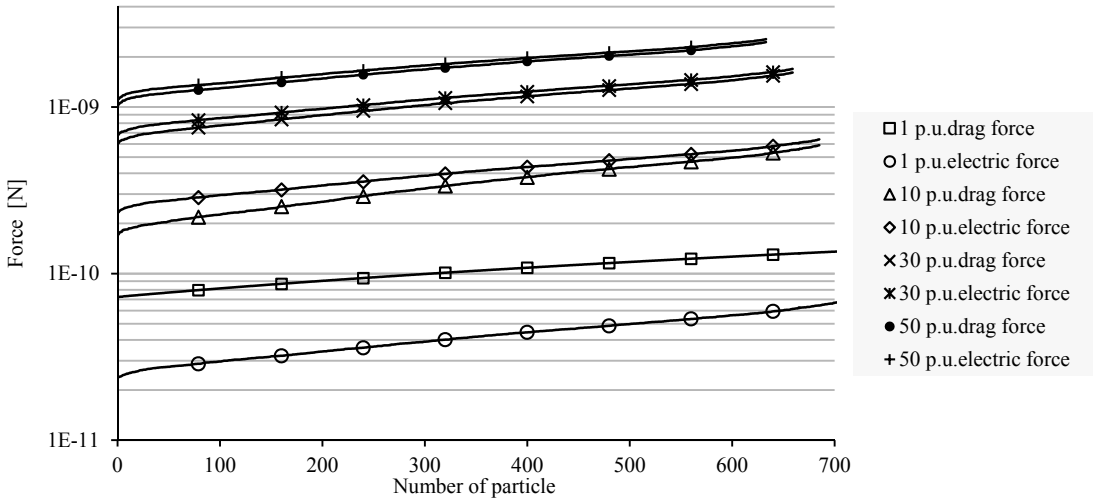

Figure 8. The curves of drag force and electric field force on the particles with different Q.

4.2. The Relationship between Charge and Particle Contact Probability

One important issue about contamination depositing is a process of contaminant particles contacting and adhering on the insulator surface. The more particles are in contact with the insulator, the greater the probability of contamination deposition is. An indirect parameter to characterize the degree of contamination was defined. It is the ratio of the number of particles in contact with the insulator surface to the total number of particles released, and named as the contact probability of particles P_{ct}.

The contact and adhesion determine the deposition of contaminant particles on the surface of insulators. The more contaminant particles that contact the insulator, the greater the accumulation of contaminant is on the surface. A ratio of number of particles contact with the insulator sheds to the total number of particles released from inlet was defined for indirectly representing the degree of contamination, and named as the contact probability of particles P_{ct}.

$$P_{ct} = N_{ct}/N_{total}, \tag{6}$$

where N_{ct} is the number of particles contact to the insulator surface, N_{total} is the total number of particles released.

The velocity of airflow V_0 was 1, 2, 3, and 5 m/s, the relationship curves between charge Q on single particle and contact probability P_{ct} are shown in Figure 9. The range of Q was from 1 p.u. to 60 p.u. It is revealed that, at low airflow velocity ($V_0 \leq 3$ m/s), the contact probability is approximately linearly increases in the front of the curve with the charge increasing. However, it decreases when the charge has a certain quantity. When the velocity of airflow from entrance reduced from 3 m/s to 1 m/s gradually, the particle charge was reduced from 30 p.u. to 10 p.u. according to the point of maximum contact probability, but the maximum contact probability still remained at about 0.011. However, when the airflow velocity reached 5 m/s, the curve of contact probability had some differences with the other curves under lower airflow velocity. At the initial stage of particle charge increasing, the contact probability increased to about 0.011 according to the particle charge 40 p.u. When the particle charge continued to increase to 60 p.u., the value of P_{ct} was still near 0.0113, and there was no downward trend.

In other previous studies [33], a deposition experiment of a scale insulator model applying DC voltage to a line conductor in test chamber was carried out. The results indicated that the average contamination on the sample insulator surface is indeed proportional to applied voltage that is shown in Figure 10. The electric field scales linearly with the applied voltage, the electric force on charged particles changes linearly, too. As in this paper, increasing the quantity of charge on particle,

the electric force also changed linearly. The curves in Figure 9, especially the linear part on the left side, have a similar shape to the curve in Figure 10.

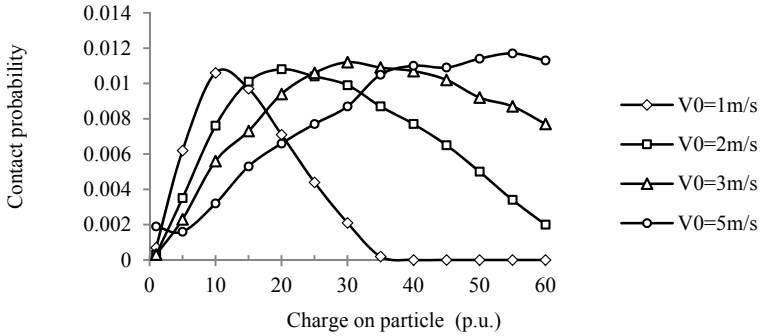

Figure 9. The relationship of electric charge on particles and particles contact probability with different airflow velocity V_0.

These characteristics can be explained in that the electric force on particle increased with the increasing of charge, while gradually performing a balance with drag force. At this moment, the particles were more easily to move to sheds that lead to the maximum value of the contact probability. As the charge increasing further, the particles were rejected away from insulator by extremely great electric force, and the number of particles near the insulator was reduced, which lead to the decrease of the contact probability. As the airflow velocity increases, more electric force is required to balance the drag force, therefore, the particle charge corresponding to maximum of contact probability under different V_0 was also increased, and the maximum of P_{ct} slightly increased near 0.011 with V_0 increasing. The role of airflow drag force on contaminant particles diminished, when the inlet velocity is reduced, the increasing charge and electric force had a more pronounced effect on the movement of particles.

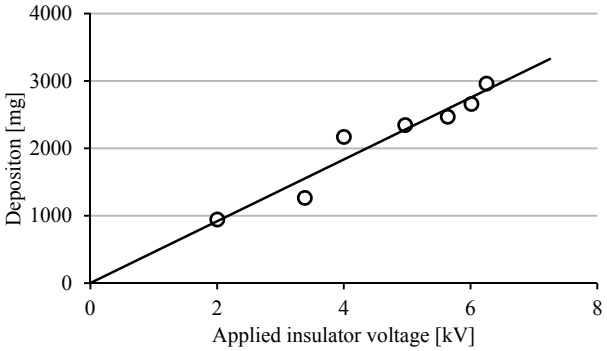

Figure 10. The relationship between deposition and applied insulator voltage [33].

5. Conclusions

By the simulation of motion of contamination particles near high voltage end of UHVDC insulator involved fluid field and electric field based on situation of simplified insulator model and uniform charging on contamination particles, the characteristics of electric force and airflow drag force on particles were analyzed. Based on the analysis of results, it can be concluded that:

1. The direction of electric force on contamination particles has obvious regularity which is always departed from the high voltage end of insulator, however, the direction of air drag force has no regularity.

2. Under these study assumptions, the airflow drag force on the contaminant particles has significantly greater magnitude than the electric force on the windward side of sheds when the quantity of electric charge on a particle is not great.
3. While charge is multiplying, the electric forces on particles have a linear increase as the growth rate of drag force is less than the electric force's. This leads to the electric force being greater than the drag force as 2 p.u. < Q < 30 p.u.; it has a trend that the magnitude of electric force is equal to drag force, both of them form a state of equilibrium as Q > 30 p.u. in the simulation of airflow entrance velocity V_0 is 3 m/s.
4. The probability of particles contacting the insulator surface increases with increasing particle charge. However, at a certain level of charge q_{ps} which has different value with different airflow velocity V_0, the contact probability has extremum here that is about 0.011. When the charge increases after exceeding the value, the contact probability decreases gradually.
5. The role of airflow drag force on contaminant particles diminishes as the velocity of airflow decreases, the increasing charge and electric force have a more pronounced effect on the movement of particles.

Acknowledgments: Research for this paper was supported by National Natural Science Foundation of China (Grant No. 51607126).

Author Contributions: Lei Lan and Gongda Zhang and Yu Wang conceived and designed the simulations; Gongda Zhang performed the simulations; all authors analyzed the data; Gongda Zhang wrote the paper, while other authors offered their modification suggestions for the manuscript.

Conflicts of Interest: The authors declare no conflict of interest.

References

1. Su, Z.Y.; Li, Q.F. Historical review and summary on measures against pollution flashover occurred in power grids in China. *Power Syst. Technol.* **2010**, *12*, 124–130.
2. Lv, F.C.; Qin, C.X.; Guo, W.Y.; Liu, Y.P. Natural contamination deposited characteristics of ±800 kV UHV DC insulators at high altitudes. *High Volt. Eng.* **2013**, *3*, 513–519.
3. Wang, S.H.; Hu, W.T.; Gong, J.G. Natural pollution accumulation characteristics of overhead transmission line insulator strings of Zhejiang electric power grid. *High Volt. Eng.* **2014**, *4*, 1002–1009.
4. Guan, Z.C.; Zhang, F.Z.; Wang, X.; Wang, L.M. Consideration on external insulation design and insulator selection of UHVDC transmission lines. *High Volt. Eng.* **2006**, *12*, 120–124.
5. Li, L.C.; Gu, Y.; Hao, Y.P. Shed parameters optimization of composite post insulators for UHVDC flashover voltages at high altitudes. *IEEE Trans. Dielectr. Electr. Insul.* **2015**, *1*, 169–176. [CrossRef]
6. Huang, Z.R.; Zhang, D.J. Development of composite insulators for 1000 kV/±800 kV AC/DC UHV transmission lines. *Power Syst. Technol.* **2006**, *12*, 87–90.
7. Leclerc, M.; Bouchard, R.P.; Gervais, Y.; Mukhedkar, D. Wetting processes on a contaminated insulator surface. *IEEE Trans. Power Appar. Syst.* **1982**, *5*, 1005–1011. [CrossRef]
8. Zhang, R.Y.; Zheng, J.C. Progress in outdoor insulation research in China. *IEEE Trans. Electr. Insul.* **1990**, *6*, 1125–1137. [CrossRef]
9. Kawai, M. Tests in Japan on the performance of salt-contaminated insulators in natural and artificial humid conditions. *Proc. Inst. Electr. Eng.* **1968**, *1*, 158–168. [CrossRef]
10. Ye, W.J.; He, W.; Li, H.Z.; Liu, G. Study on a dynamic model of pollution particles on the near surface of electric external insulation under low wind speed condition. *Insul. Surg. Arresters* **2012**, *6*, 19–25.
11. Jiang, X.L.; Li, H.B. Application of computational fluid dynamics to analysis of contamination depositing characteristics of insulators. *High Volt. Eng.* **2010**, *2*, 329–334.
12. Sun, J.X.; Xu, Y.; Hu, X.Y. Characteristics of pollution distribution on insulators nearby electrified railroad in high-speed aerosol. *High Volt. Eng.* **2014**, *1*, 95–102.
13. Wang, J.; Chen, L.H.; Liu, Y.; Liang, X.D. Effect of the electric field on the contamination accumulation characteristic of the insulators. *High Volt. Eng.* **2011**, *3*, 585–593.

14. Sun, B.Q.; Wang, L.M.; Guan, Z.C. Influence of voltage types and polarity on contamination of insulators. *High Volt. Eng.* **2013**, *12*, 3101–3108.
15. Liu, Z.H. Research on the Ionized Field and Insulator Pollution of HVDC Transmission Lines under Haze Weather. Ph.D. Thesis, Chongqing University, Chongqing, China, 2014.
16. Ravelomanantsoa, N.; Farzaneh, M.; Chisholm, W.A. A simulation method for winter pollution contamination of HV insulators. In Proceedings of the 2011 Electrical Insulation Conference (EIC), Annapolis, MD, USA, 5–8 June 2011; pp. 373–376.
17. Ravelomanantsoa, N.; Farzaneh, M.; Chisholm, W.A. Insulator pollution processes under winter conditions. In Proceedings of the 2005 Annual Report Conference on Electrical Insulation and Dielectric Phenomena, Nashville, TN, USA, 19 December 2005; pp. 321–324.
18. Horenstein, M.N.; Melcher, J.R. Particle contamination of high voltage DC insulators below corona threshold. *IEEE Trans. Electr. Insul.* **1979**, *14*, 297–305. [CrossRef]
19. Olsen, R.G.; Daffe, J. The effect of electric field modification and wind on the HVDC insulation contamination process. In Proceedings of the IEEE Power Apparatus and System Winter Conference, New York, NY, USA, 29 January–3 February 1978.
20. Li, H.Z. Study on the Mechanism of Dynamic Contamination Accumulating and its On-Line Monitoring of External Insulation of High Voltage Transmission Line. Ph.D. Thesis, South China University of Technology, Guangzhou, China, 2013.
21. Wang, L.M.; Liu, T.; Mei, H.W.; Xiang, Y. Research on contamination deposition characteristics of post insulator based on computational fluid dynamics. *High Volt. Eng.* **2015**, *8*, 2741–2749.
22. Li, M.X. Contamination Characteristics and Electric Field Distribution of Roof Insulators on High Speed Train. Master's Thesis, Southwest Jiaotong University, Chengdu, China, 2013.
23. Yuan, Z.L.; Zhu, L.P. *Gas Solid Two Phase Flow and Numerical Simulation*; Southeast University Press: Nanjing, China, 2013; pp. 33–47.
24. Xie, G.R. *High Voltage Electrostatic Precipitation*; Water Resources and Electric Power Press: Beijing, China, 1993; pp. 28–49.
25. Deng, T.; Su, Z.Y.; Fan, J.B.; Li, Q.F. Design optimization of grading ring of composite insulators for ±800 kV UHVDC line. *Power Syst. Technol.* **2010**, *8*, 31–35.
26. Guo, F.; Liu, S.T.; Li, X.G. Component analysis of insulator contaminant in typical environment of Ningxia province. *Insul. Mat.* **2017**, *4*, 61–66.
27. Bogoroditsky, N.P.; Pasynkov, V.V.; Tareev, B.M. *Electrical Engineering Materials*; Mir Publishers: Moscow, Russia, 1979; pp. 195–198.
28. Lu, T.B.; Feng, H.; Zhao, Z.B. Analysis of the electric field and ion current density under ultra-high-voltage direct-current transmission lines based on finite element method. *IEEE Trans. Magn.* **2007**, *43*, 1221–1224. [CrossRef]
29. Zhou, X.X.; Cui, X.; Lu, T.B. Spatial distribution of ion current around HVDC bundle conductors. *IEEE Trans. Power Deliv.* **2012**, *27*, 380–390. [CrossRef]
30. Cai, W.; Xiao, Y.; Wu, G.Y. Elementary analysis of pollution rules of insulators on ±500 kV DC transmission lines. *High Volt. Eng.* **2003**, *6*, 4–5.
31. Su, Z.Y.; Liu, Y.S. Comparison of natural contaminants accumulated on surfaces of suspension and post insulators with dc and ac stress in northern China's inland areas. *Power Syst. Technol.* **2004**, *10*, 13–17.
32. Wang, B.; Liang, X.D.; Zhang, Y.B. Natural pollution test of composite and porcelain insulators under AC and DC stress. *High Volt. Eng.* **2009**, *9*, 2322–2328.
33. Horenstein, M.N. Particle Contamination of High Voltage DC Insulators. Ph.D. Thesis, Massachusetts Institute of Technology, Cambridge, MA, USA, 1978.